Polar Three-Arm Star Block Copolymer Thermoplastic Elastomers Based on Polyacrylonitrile

Bruno Dufour,[†,⊥] Chuanbing Tang,[†,§] Kaloian Koynov,*[,‡] Ying Zhang,[‡] Tadeusz Pakula,[‡,#] and Krzysztof Matyjaszewski*[,†]

Center for Macromolecular Engineering, Department of Chemistry, Carnegie Mellon University, 4400 Fifth Avenue, Pittsburgh, Pennsylvania 15213, and Max-Planck-Institut for Polymer Research, P.O. Box 3148, D-55021 Mainz, Germany

Received November 18, 2007; Revised Manuscript Received January 14, 2008

ABSTRACT: A series of well-defined poly(*n*-butyl acrylate)-*b*-polyacrylonitrile (PBA−PAN) triarm star block copolymers have been synthesized by ATRP. The incorporation of very polar hard segment of PAN was made possible with the aid of the halogen-exchange technique. Phase-separated morphology of cylindrical PAN domains hexagonally arranged in the pBA matrix was observed by atomic force microscopy and small-angle X-ray scattering in all studied materials. The mechanical and thermal properties of the PBA−PAN triarm star block copolymers have been thoroughly characterized, and their thermoplastic elastomer behavior was studied. It was found that these block copolymers retain a phase-separated morphology until temperatures of at least 250 °C. Furthermore, because of chemical cross-linking of the PAN segments that takes places at around 280 °C, the triarm star PBA-PANs preserve their elastomeric properties until temperatures of more than 300 °C.

Introduction

Thermoplastic elastomers (TPE) are an important class of materials combining elastomeric behavior with thermoplastic properties.[1−3] Typically, these are ABA triblock copolymers exhibiting strong phase separation in the bulk state. The hard phase formed from the component A is dispersed in the continuous soft rubbery matrix of component B serving as a physical cross-linker. The polystyrene−polyisoprene−polystyrene (SIS) and polystyrene−polybutadiene−polystyrene (SBS) triblock copolymers are probably the best known examples of such thermoplastic elastomers[1−3] that have been commercially used. However, these materials contain unsaturated double bonds in the middle segments, which make them susceptible to oxidation and eventually reduce the lifetime of usage.[4,5]

Thus, continuous efforts have been devoted to change outer and inner segments of ABA triblock copolymers[6−8] or design new types of materials bearing novel architectures and topology,[9,10] which require development of new synthetic techniques. Traditionally, many TPE have been prepared using living ionic polymerizations as well documented in the literature.[11−20] However, these strategies require stringent conditions and are intolerant of water, air, impurities, and a lot of functionality and polarity. In the past decade, controlled/living radical polymerization (CRP) has emerged as an excellent tool to synthesize materials with controlled molar mass, narrow molecular weight distribution, and well-defined architectures and functionalities.[21−28] Atom transfer radical polymerization (ATRP) and other CRP techniques are compatible with a wide range of monomers including polar and nonpolar monomers such as acrylates, methacrylates, acrylonitrile, and styrene.[29−36] In the recent years, CRP techniques have been introduced to synthesize materials used as TPE.[37−52] Using CRP techniques, it is possible to substitute traditional unsaturated middle segment by acrylates and hard segments by methacrylates or acrylonitrile-based block copolymers. This would enable many benefits ranging from flexible glass transition temperatures (−60 to 200 °C), to better oxidation resistance, and to resistance to hydrocarbons, opening new applications e.g. in the automotive market.

Recently, our group reported successful one-pot synthesis of triblock copolymers poly(methyl methacrylate)-*b*-poly(*n*-butyl acrylate)-*b*-poly(methyl methacrylate) (PMMA−PBA−PMMA), fully acrylic thermoplastic elastomers, by using copper-base catalyst and halogen exchange to achieve reasonably low polydispersity.[39] The absence of double bonds in these fully acrylic TPEs is an important improvement in terms of light sensitivity and oxidation stability. Jerome and co-workers also used ATRP to synthesize PMMA−PBA−PMMA block copolymers in the presence of $NiBr_2(PPh3)_2$ catalyst with and without using the halogen-exchange technique.[38,53−55] While both materials displayed typical thermoplastic elastomer properties, the maximum elongation at break and ultimate tensile strength were relatively low. This was related to higher polydispersity and plausible inefficient cross-propagation, since fully acrylic TPEs synthesized by ionic polymerizations produced better mechanical properties.[8,55] The issue could be also attributed to large molecular weight between chain entanglements (M_e) for the middle rubbery block of PBA.[16]

During the past several years it was demonstrated that thermoplastic elastomers based on star block copolymers[9,56−59] may exhibit superior properties as compared to the linear ABA triblock copolymer type TPEs. It was reported that multiarmed polystyrene-*b*-polyisobutylene (PS-*b*-PIB) star block copolymers have substantially better mechanical properties and much lower sensitivity to diblock contamination than their linear triblock counterparts.[58]

Herein we report the synthesis of triarm star block copolymer thermoplastic elastomers, which comprise poly(*n*-butyl acrylate)-*b*-polyacrylonitrile (PBA−PAN) arms. The incorporation of very polar hard segment of PAN was possible with the aid of the halogen-exchange ATRP technique.[60,61] We have studied the structure and the mechanical properties of the PBA−PAN star block copolymers and found that they exhibit thermoplastic elastomer characteristics. In that respect this is the first comprehensive study of star copolymer TPEs prepared by CRP.

* To whom correspondence should be addressed.
† Carnegie Mellon University.
‡ Max-Planck-Institut for Polymer Research.
§ Current address: Materials Research Laboratory, University of California, Santa Barbara, CA 93106.
⊥ Current address: Corning SAS, Corning European Technology Center, 77210 Avon, France.
Deceased June 7, 2005.

10.1021/ma702561b CCC: $40.75
Published on Web 02/23/2008

Scheme 1. Synthesis of 3-Arm Star PBA-*b*-PAN Block Copolymers

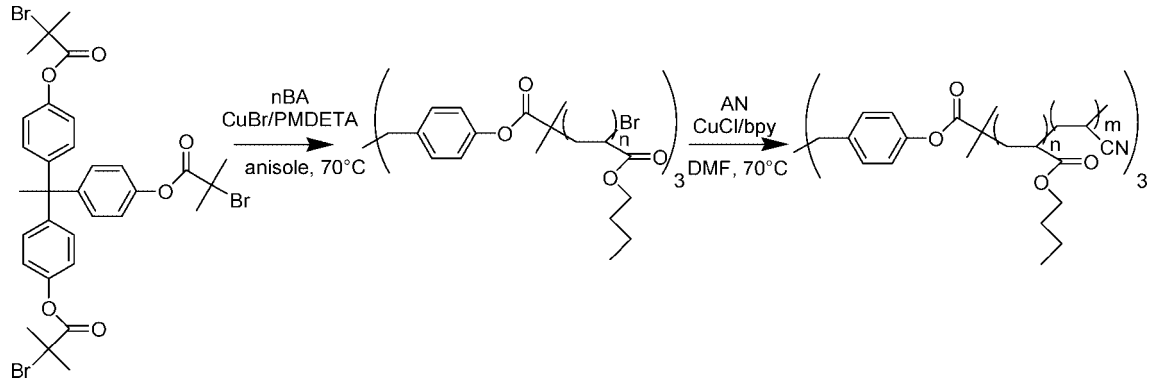

Moreover, PBA−PAN star copolymers are of particular interest as they can be potentially used to fabricate organized nanostructured carbon materials after thermal pyrolysis.[22,37,62–65]

Experimental Section

Materials. *n*-Butyl acrylate (BA) and acrylonitrile (AN) were purchased from Aldrich and distilled under vacuum. Cu(I)Br and Cu(I)Cl were obtained from Aldrich and purified according to published procedures.[15,66] 4,4′-Di(5-nonyl)-2,2′-bipyridine (dNbpy) was prepared as described elsewhere.[67] *N,N,N′,N″,N″*-Pentamethyldiethylenetriamine (PMDETA), $CuCl_2$, 2,2′-bipyridine (bpy), anisole, and methanol were used as received from Aldrich. 1,1,1-Tris(4-(2-bromoisobutyryloxy)phenyl)ethane was synthesized according to the literature.[68,69]

Synthesis of 3-Arm Bromo-Terminated Poly(*n*-butyl acrylate) (PBA) Macroinitiator. In a typical experiment 50 mg of 1,1,1-tris(4-(2-bromoisobutyryloxy)phenyl)ethane (0.067 mmol) and 20.1 μL of pentamethyldiethylenetriamine (0.1 mmol) were dissolved in 10 mL of deoxygenated butyl acrylate and 1.5 mL of deoxygenated anisole that had been added to a 25 mL Schlenk flask. 14.3 mg of CuBr (0.1 mmol) was then added under nitrogen flow, and then the flask was heated to 70 °C for 18 h to conduct the polymerization. The contents of the flask were diluted with THF, passed through a neutral alumina column, and dried under vacuum until constant weight. By adjusting the ratio of concentrations of monomer to initiator, five PBA macroinitiators were prepared with M_n = 19 800, 63 000, 87 000, 117 000, 148 800, and 210 000 and with polydispersities M_w/M_n = 1.13, 1.12, 1.17, 1.19, 1.17, and 1.25, respectively, according to Scheme 1.

Synthesis of 3-Arm Star PBA-*b*-PAN. In a typical experiment, 1 g of a 3-arm bromo-terminated poly(butyl acrylate) macroinitiator (M_n = 117 000 g/mol and M_w/M_n = 1.19) and 2,2′-bipyridine were dissolved in deoxygenated DMF/acrylonitrile (50/50 vol %) under a nitrogen atmosphere in a 25 mL Schlenk flask. Copper chloride was then added under nitrogen flow. The reaction was carried out at 70 °C for 3 h. The polymer was precipitated by addition to 200 mL water/methanol mixture, washed three times with 100 mL water/methanol, filtered, and dried until constant weight.

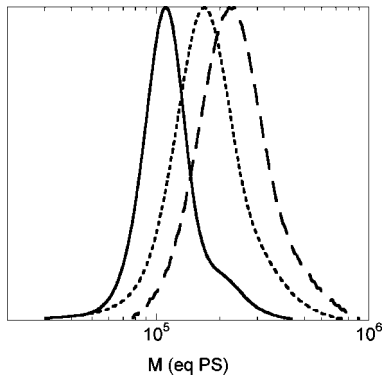

Figure 1. GPC traces of T-PBA304-PAN109, 13 wt % PAN (- - -), T-PBA304-PAN207, 22 wt % PAN (— —), and the corresponding 3-arm star poly(butyl acrylate) macroinitiator T-PBA304 (—).

Preparation of Films of 3-Arm Star PBA-*b*-PAN Block Copolymers. Thick films were obtained by casting of 20 wt % star polymers in DMF on glass plate followed by removal of the solvent at room temperature under vacuum. Free-supported films were removed from the substrate in methanol/water mixture. Films were then dried under vacuum until constant weight. The final film thickness was on the order of 0.25 mm. For TMAFM measurements, thin (<500 nm) films were obtained by spin-casting 10 mg/mL polymer solutions in DMF onto silicon wafer substrates followed by removal of the solvent under vacuum.

General Analysis. Size exclusion chromatography (SEC) was conducted using DMF as the eluent (flow rate 1 mL/min, 50 °C) with a series of three Styrogel columns (105 Å, 103 Å, 100 Å; Polymer Standard Services) and a Waters 2410 differential refractometer. Toluene was used as the internal standard. Polystyrene standards were employed for the SEC calibration. Elemental analysis was performed by Midwest Microlab LLC. Differential scanning calorimetry (DSC) measurements were performed using a Mettler DSC 30 apparatus at a temperature variation rate of 10 °C/min for both heating and cooling runs.

Dynamic Mechanical Analyses (DMA). DMA have been performed using a Rheometrics RMS 800 mechanical spectrometer. Shear deformation was applied under conditions of controlled deformation amplitude, which was kept in the range of the linear viscoelastic response of studied samples. Plate−plate geometry was used with plate diameters of 6 mm. Experiments have been performed under a dry nitrogen atmosphere. Results are presented as temperature dependencies of the storage (G') and loss (G'') shear modulus measured at a constant deformation frequency of 10 rad/s. The results were obtained with a 2 °C/min heating rates.

Tensile Tests. Measurements were performed using a mechanical testing machine Instron 6000. Samples having the thickness of about 0.2 mm have been drawn with the rate of 5 mm/min at room or at elevated temperatures. Dependencies of stress vs draw ratio were recorded. Elastic modulus, elongation at break, and stress at break have been determined as averages of 3–5 independent drawing experiments performed at the same conditions.

Small-Angle X-ray Scattering (SAXS) Analyses. SAXS measurements were conducted using a rotating anode (Rigaku RA-Micro 7) X-ray beam with a pinhole collimation and a two-dimensional detector (Bruker Highstar) with 1024 × 1024 pixels. A double graphite monochromator for the Cu Kα radiation (λ = 0.154 nm) was used. The beam diameter was about 0.8 mm, and the sample-to-detector distance was 1.8 m. The recorded scattered intensity distributions were integrated over the azimuthal angle and are presented as functions of the scattering vector ($s = 2\sin(\theta)/\lambda$, where 2θ is the scattering angle).

Tapping Mode Atomic Force Microscopy (TMAFM). TMAFM studies were carried out with the aid of a NanoScope III-M

Table 1. Series of 3-Arm Star PBA−PAN Block Copolymers

sample	arm composition	M_n PBA 3-arm star (g/mol)	M_n PBA-PAN 3-arm star (g/mol)	PAN (wt %)	M_w/M_n
T-PBA304-PAN63	$(BA_{304}$-*b*-$AN_{63})_3$	117000	127000	8	1.14
T-PBA304-PAN109	$(BA_{304}$-*b*-$AN_{109})_3$	117000	134300	13	1.17
T-PBA304-PAN207	$(BA_{304}$-*b*-$AN_{207})_3$	117000	149900	22	1.17
T-PBA304-PAN331	$(BA_{304}$-*b*-$AN_{331})_3$	117000	169600	31	1.11
T-PBA388-PAN115	$(BA_{388}$-*b*-$AN_{115})_3$	148800	167000	11	1.07
T-PBA388-PAN165	$(BA_{388}$-*b*-$AN_{165})_3$	148800	175000	15	1.13
T-PBA388-PAN264	$(BA_{388}$-*b*-$AN_{264})_3$	148800	190800	22	1.15
T-PBA52-PAN26	$(BA_{52}$-*b*-$AN_{26})_3$	19800	23900	17	1.22
T-PBA547-PAN153	$(BA_{547}$-*b*-$AN_{153})_3$	210000	234300	10	1.16

Scheme 2. Geometries Employed in SAXS Analysis: (Left) X-Ray Beam Is Perpendicular to the Film Surface, T Geometry; (Right) X-ray Beam Enters the Film from the Side, S Geometry

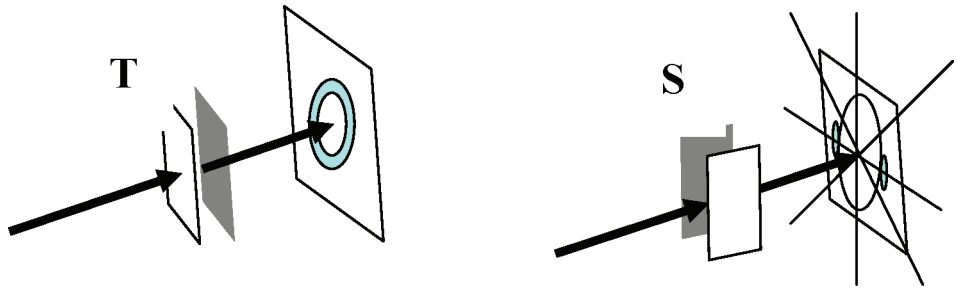

system (Digital Instruments, Santa Barbara, CA), equipped with a J-type vertical engage scanner. TMAFM observations were performed at room temperature in air using silicon cantilevers with nominal spring constant of 40 N/m and nominal resonance frequency of 300 kHz (standard silicon TESP probes).

Results and Discussion

Synthesis. Synthesis of 3-arm star PBA−PAN block copolymers involved the use of halogen-exchange strategy, which significantly improved chain-extension efficiency.[61,70] An example of evolution of GPC traces of block extension from a poly(butyl acrylate) 3-arm star with DP 304 (117 000 g/mol) with polyacrylonitrile segments is reported in Figure 1. A smooth shift of the entire molecular weight distribution was observed. Neither unreacted poly(butyl acrylate) macroinitiator nor homopolyacrylonitrile could be observed. The compositions of the prepared 3-arm poly(butyl acrylate)-*block*-polyacrylonitrile copolymers were determined by elemental analysis and are given in Table 1. All copolymers had low polydispersities, as reported in Table 1.

Morphology. Because of the strong incompatibility between the two phases, the PBA−PAN star copolymers are expected to show very strong phase separation. In an attempt to visualize this effect, we have performed AFM imaging on thin films prepared by spin-casting of polymer solutions in DMF onto silicon wafer substrates. Phase contrast imaging of AFM enables visualization of different microdomains with the aid of pronounced difference of mechanical (e.g., viscoelastic) properties of block copolymer components. The phase shift is primarily dictated by the amount of energy dissipated through tip–sample interactions. Normally, viscous components induce more energy dissipation during tip–sample interactions, yielding more phase shift and generally appearing darker in the phase images.[71,72] Rigid PAN components (therefore less energy dissipated) and much softer PBA components (therefore more energy dissipated) would provide sufficient elasticity difference to impart strong contrast in the phase imaging. Typical results are shown in Figure 2. As can be seen in the figure, the phase contrast AFM images of the films reveal the phase-separated morphology of 3-arm star PBA−PAN block copolymers. Rigid PAN domains (brighter features in AFM images) are dispersed in the softer PBA matrix. The sample with lowest content of PAN (8 wt %) shows round features, while the sample with 13 wt % PAN displays a mixture of round and elongated (cylindrical) features. As the round features may originate from either spheres or standing-up cylinders, other experimental techniques (e.g., SAXS as described below) are needed to unambiguously determine the film morphology. Finally, the sample with highest PAN content (22 wt %) displayed meandering curved features, characteristic for short-range ordered cylindrical structures or bicontinuous structures (the latter would be less plausible since bicontinuous structures are more likely to be suppressed in thin films).

In order to get a better insight into the morphology of PBA−PAN films, they were analyzed by SAXS in two different geometries: (i) with the X-ray beam going through (T) the film and (ii) with the X-ray beam entering the film from the side (S), as shown in Scheme 2.

First, X-ray scattering experiments were carried out with as-cast films, i.e., without thermal treatment. The results for the sample with lowest content of PAN (T-PBA304-PAN63: 8 wt % PAN) are shown in Figure 3. Unfortunately, only two relatively well-defined scattering peaks are observed in both S and T configurations that make the unambiguous determination of the morphology rather difficult. The main reason for this is the very small difference in the electron density between the PBA and PAN components that leads to a low scattering efficiency. The AFM study of this copolymer morphology (Figure 2) has revealed round features that may originate either from spheres or a cylinders perpendicular to the film surface. A body-centered-cubic (bcc) structure typically observed for spherical morphology should produce a series of peaks with s ratios $1{:}\sqrt{2}{:}\sqrt{3}$. Alternatively, a hexagonally packed cylinders would produce peaks with s ratios $1{:}\sqrt{3}{:}\sqrt{4}$. As marked in Figure 3, our SAXS data reveal two scattering maxima situated at relative positions $1s$ and $\sqrt{3}s$, which is consistent with the cylindrical morphology. At the same time we cannot exclude the existence of a weak ill-resolved peak at $\sqrt{2}s$ and therefore the spherical morphology.

As shown in Figure 4, the SAXS patterns in both T and S geometries reveal the formation of cylindrical structures (two scattering peaks at s and $\sqrt{3}s$) in the sample with moderate PAN content (T-PBA304-PAN109: 13 wt % PAN). Comparison of the T and S geometries patterns indicates formation of a

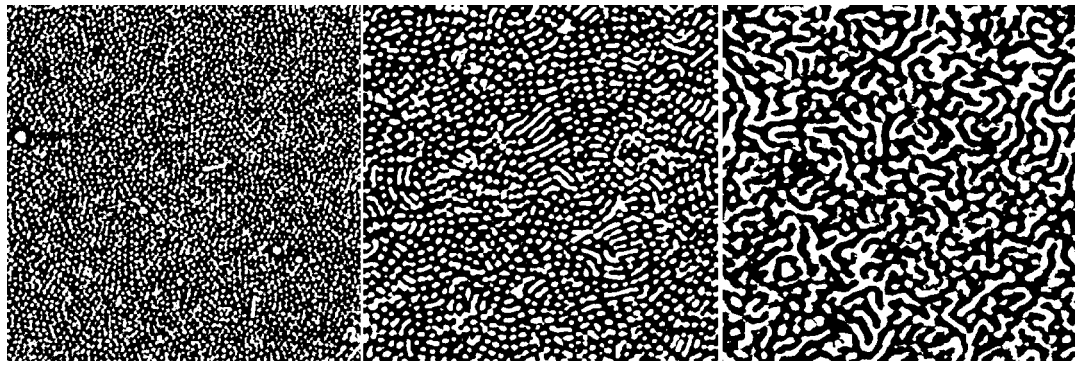

Figure 2. AFM phase images of 3-arm star PBA−PAN block copolymers: (left) T-PBA304-PAN63 (8 wt % PAN); (middle) T-PBA304-PAN109 (13 wt % PAN); and (right) T-PBA304-PAN207 (22 wt % PAN). Image size: 2 μm × 2 μm.

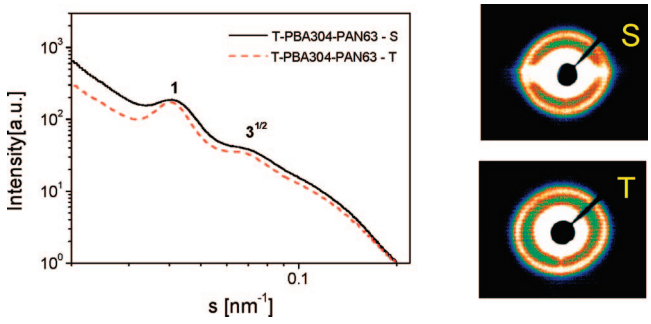

Figure 3. SAXS from film of star copolymers T-PBA304-PAN63 (8 wt % PAN).

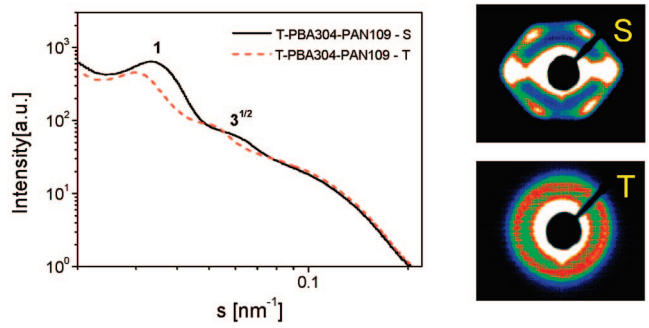

Figure 4. SAXS from film of star copolymers T-PBA304-PAN109 (13 wt % PAN).

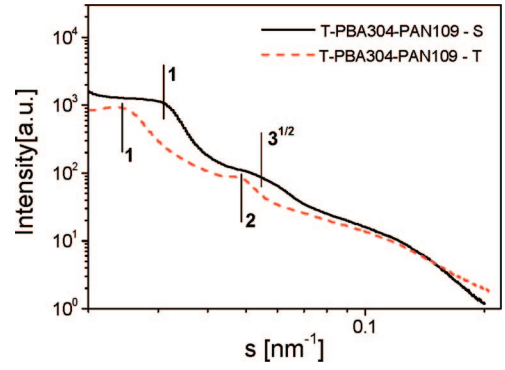

Figure 5. SAXS from film of star copolymers T-PBA304-PAN109 (22 wt % PAN).

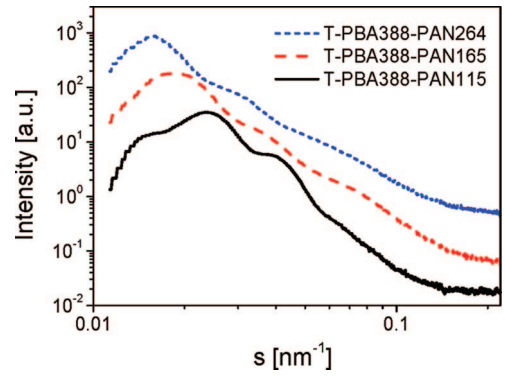

Figure 6. SAXS spectra of 3-arm star PBA-*b*-PAN with constant PBA segments length and increasing PAN length. Measurements were done in (S) geometry.

mixture of perpendicular and parallel to the film surface cylinders, with domination of the former ones. These structural arrangements agreed well with the AFM observations (Figure 2).

The SAXS spectra of the as cast films of the star block copolymers with higher PAN content (T-PBA304-PAN207: 22 wt % PAN) showed a very shallow high-order peaks that do not allow assigning of a specific morphology. We have therefore studied the same film after annealing for 2 h at 150 °C. The results are shown in Figure 5. As can be seen, the thermal annealing has resulted in a better distinguished secondary peaks. When the SAXS experiments were performed in T configuration, the ratio of the scattering vectors of the peaks was again 1:$\sqrt{3}$, revealing a cylindrical morphology. For the experiments performed in S configuration, scattering peaks were observed at 1*s* and 2*s*, which may suggest the presence of lamella morphology as well. Again, these results while not completely conclusive are in a good agreement with the AFM data shown in Figure 2.

We have performed similar SAXS experiments with all PBA−PAN copolymers listed in Table 1. While most of them revealed similar cylindrical morphologies, their different compositions affect the cylinders *d*-spacing in the microphase-separated structures. As shown in Figure 6, the increase of PAN block length leads to an increase in the *d*-spacing at the same length of the PBA segment. We have also studied the effect of thermal treatment on the morphology of several PBA−PAN star copolymers and found that while the annealing does not change the type of microstructure it leads to a better defined SAXS patterns.

Dynamic Mechanical Properties. The dynamic mechanical properties of the PBA−PAN star copolymers were characterized through the temperature dependencies of the real (G') and the imaginary (G'') parts of the complex shear modulus. Some typical results for a series of copolymers with constant PBA content (DP equal to 304) and varying PAN fractions are shown in Figures 7 together with the respective DSC thermographs. As can be seen in every case, four major transitions were

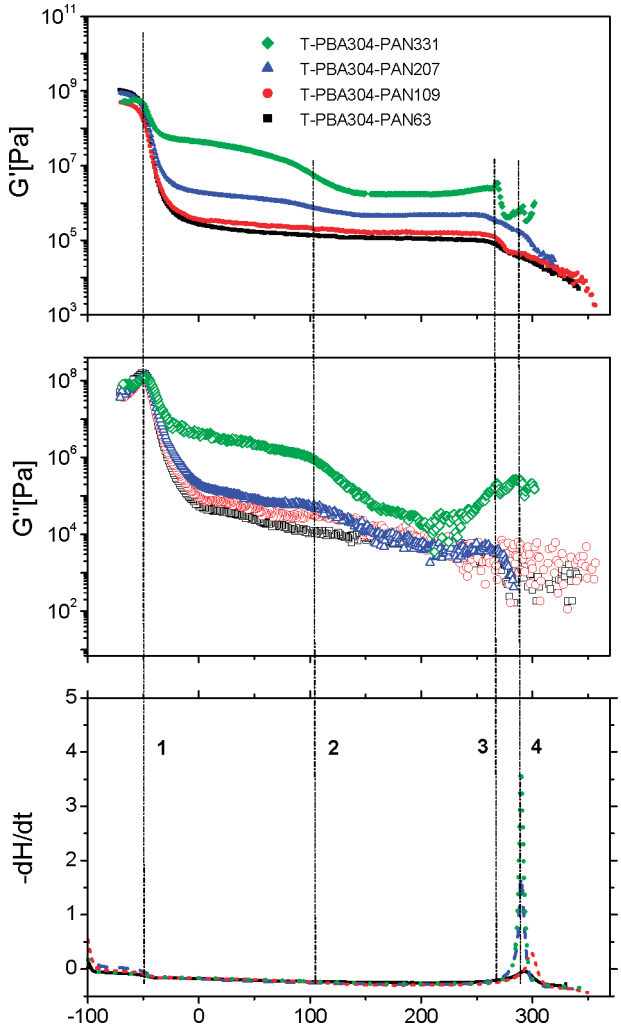

Figure 7. Thermomechanical (2 °C/min) and DSC (10 °C/min) analysis of 3-arm star PBA-*b*-PAN copolymers.

observed. The first two correspond to the glass transitions of PBA (∼–50 °C) and PAN (∼105 °C). The third transition, at temperatures around 260 °C, manifests itself by a rather sharp drop in the storage modulus G'. Finally, at higher temperatures (280–290 °C) an exothermal process is observed in the DSC thermographs with intensity proportional to the content of PAN in the material. This process is related to chemical cross-linking of the PAN segments.

With respect to the mechanical properties, all samples were glassy below the glass transition temperature of PBA, with storage modulus $G' \sim 1$ GPa. Above this glass transition, the copolymers become elastic and show a G' plateau extending up to the softening temperature of PAN (∼100 °C). The height

Table 2. Mechanical Properties of PBA−PAN Triarm Star Block Polymers with Various Compositions[a]

sample	PAN (wt %)	E/MPa	λ_{break}	σ_{break}/MPa
T-PBA304-PAN63	8	0.37	4.23	1.27
T-PBA304-PAN109	13	0.67	4.59	4.85
T-PBA304-PAN207	22	6.58	4.19	10.0
T-PBA304-PAN331	31	71.0	3.75	15.4
T-PBA388-PAN115	11	0.57	6.0	6.8
T-PBA388-PAN165	15	1.8	4.4	6.3
T-PBA388-PAN264	22	6.8	3.82	12.7

[a] E = initial tensile modulus, λ_{break} = draw ratio at break, and σ = stress at break.

of the plateau dependents strongly on the PAN content: $G' \sim 0.1$ MPa when PAN fraction <0.1 and $G' \sim 100$ MPa when PAN fraction is 0.3. In this elastic state the PAN blocks form the glassy domains connecting the flexible PBA blocks. This corresponds to a typical situation for a thermoplastic elastomer in which the hard phase elements (i.e., the glassy microdomains) act as physical cross-links for the flexible component. Both storage and loss moduli decrease above the T_g of PAN, but a second plateau with lower G' values (0.1–1 MPa) extends until temperatures of ∼260 °C. It is well-known that the classical SBS and SIS thermoplastic elastomer systems exhibit phase separation that may persist beyond the upper (PS) glass transition temperature.[2] However, above a certain temperature, the phase separation disappears and a monophase fluid is formed. This order–disorder transition (ODT) process is observed for most block copolymers.[73–77] For example, in their extensive work on the MAM triblock copolymer thermoplastic elastomers,[18,51,78,79] Jerome et al. have shown that depending on the degree of miscibility of PMMA with poly(alkyl acrylate)s the ODT temperature in these systems may exceed 200 °C. In this respect the results shown in Figure 7 demonstrate that the 3-arm star PBA-*b*-PAN copolymers maintain their microdomain morphology up to a very high ODT temperature of around 260 °C, i.e., ∼150 °C above the glass transition of the PAN.

At even higher temperatures the storage modulus start to decrease again, but no flow is observed in the entire temperature range studied, i.e., up to 330 °C. This interesting effect is most likely related to the fourth transition shown in Figure 7, namely, the chemical cross-linking of the PAN segments. This process takes place at around 280–290 °C (i.e., slightly above the ODT) and, above a certain temperature, becomes the predominant factor that prevents the system from flowing. In the sample with the highest PAN content T-PBA304-PAN331 (31 wt %) even a further increase of G' at higher temperatures is observed. In this way the chemical cross-linking of the PAN segments results in a conversion of the material from TPE to a chemically cross-linked elastomer after temperature treatment. Because of this effect, the 3-arm star PBA−PAN block copolymers retain their elastomeric properties until temperatures of more than 300 °C.

A careful examination of Figure 7 shows that one additional process seems to take place in the copolymer with the highest

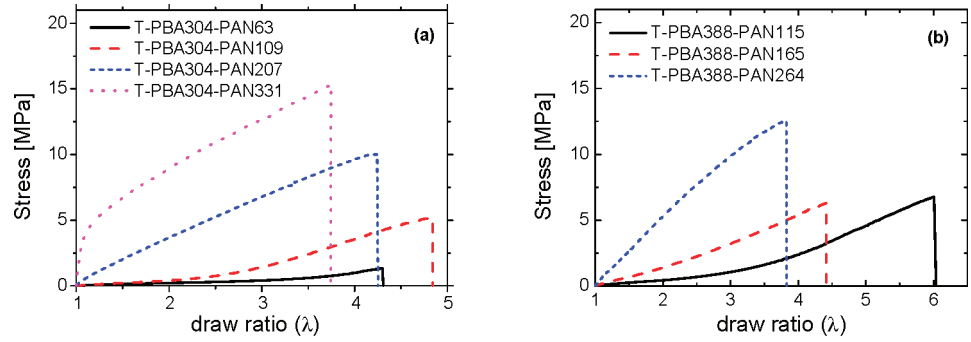

Figure 8. Stress−strain curves recorded for PBA−PAN star copolymers with varying content of PAN for same length of PBA.

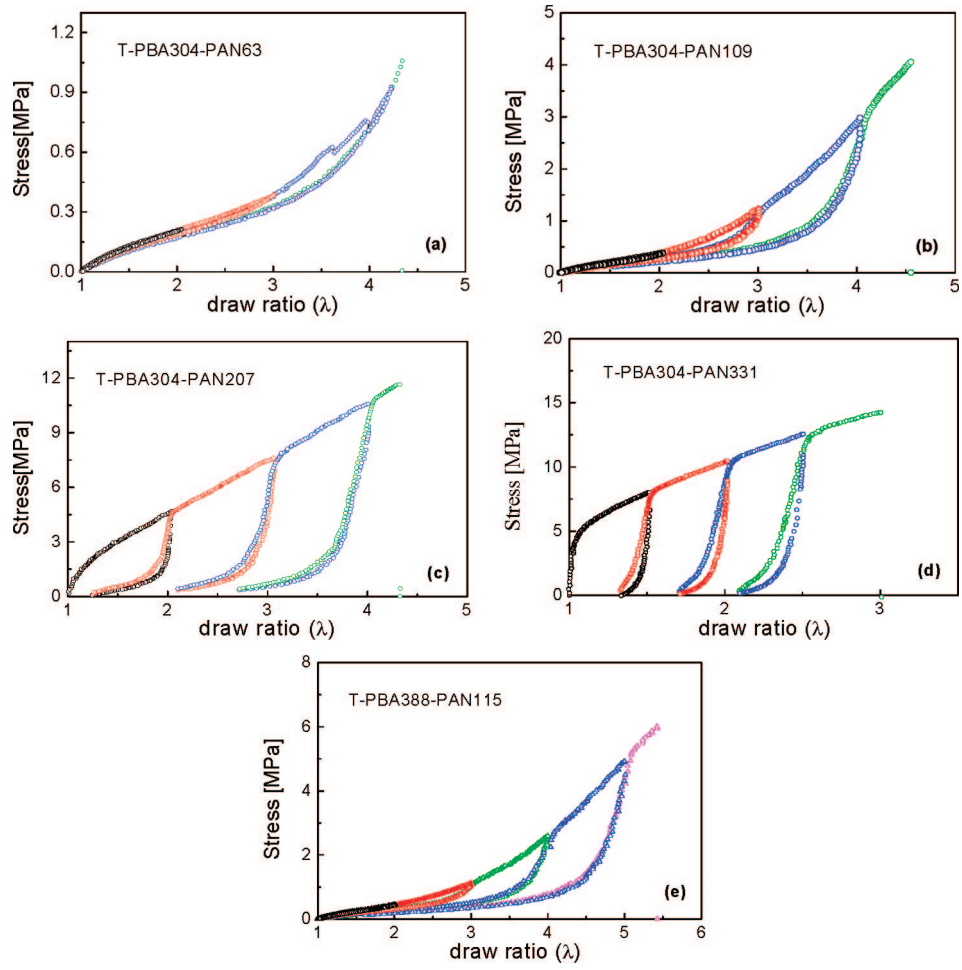

Figure 9. Quasi-static stress–strain cycles of PBA-PAN star copolymers with different PAN content: (a) 8, (b) 13, (c) 22, and (d) 31, and (e) 11 wt %.

PAN content (T-PBA304-PAN331, 31 wt %) starting at temperature of around 200 °C. The process is characterized by an increase in G' and in particular in G''. One possible cause of this transition may be a rearrangement in the sample morphology, e.g., from cylindrical to a lamella or bicontinuous type of microstructure. Such types of rearrangements are known as order to order transitions (OOT) and have been observed in other copolymer systems.[80–82] However, further studies including high-temperature SAXS are needed to explore this process in greater detail.

Tensile Mechanical Properties. The tensile mechanical properties of the PBA−PAN star copolymers were also investigated, and some typical results are shown in Figure 8. Clearly the studied samples show a behavior typical for elastomeric materials with elongations at break up to 500% and stress at break up to 15 MPa.

The basic tensile mechanical characteristics of all copolymers studied are summarized in Table 2. As expected, the composition has a major effect on the tensile properties of the PBA−PAN star copolymers. The data show that both the initial modulus (E) and the tensile strength (σ_{break}) increase strongly with PAN content, while the draw ratio at break seems to increase with the length of pBA segment and be reduced with increasing PAN content. These findings suggest an easily way for tuning the material properties by adjusting the copolymers composition.

We should emphasize at this point that both ultimate tensile strength and elongation at break of the PBA−PAM 3-arm star block copolymers reported in Table 2 are significantly lower than those of the classical SIS and SBS thermoplastic elastomers with comparable molecular weights. While problems with the synthesis of the PBA−PAM stars such as incomplete functionalization or relatively high polydispersity may decrease their tensile properties, there is also a more important fundamental reason for this difference. As discussed by Tong and Jeromy,[17] the molecular weight between chain entanglements, M_e, of the soft PBA block is much higher than those of the central polybutadiene/polyisoprene blocks in the SBS/SIS. In this way, since the number of chain entanglements is limited in the PBA−PAM systems, the deformation stress is not dissipated by the soft PBA block but directly transferred to the hard PMA microdomains.

In order to further explore the elastomeric properties of the PBA−PAN star copolymers, we have also studied their performance at large deformations. Figure 9 shows typical plots resulting from quasi-static stress–strain cycles with successively increasing maximum strain. The copolymer composition has a major effect on the material properties. The T-PBA304-PAN63 sample which has a low PAN content (8 wt %) exhibited nearly ideal elastic behavior: no residual strains after unloading. When the PAN content was increased to 13 wt %, as shown in Figure 9b, the deformations were still reversible, but the modulus was lowered after application of each stress–strain cycle. When the PAN content was increased to 22 wt % and further to 31 wt %, as shown in Figure 9c,d, the effect of stretching the materials was clearly irreversible, and the modulus was strongly reduced after each application of stress. These samples showed elastoplastic behavior, i.e., large residual strains after unloading, which is probably associated with fragmentation of the cylindrical PAN

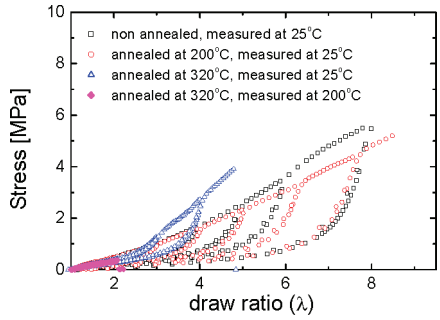

Figure 10. Tensile mechanical properties of the star copolymer T-PBA388-PAN115. The annealing at 200 °C was done for 30 min and at 320 °C for 10 min.

domains. Sample T-PBA388-PAN115 with longer PBA arm (388 vs 304) but a PAN content similar to T-PBA304-PAN109 (11 vs 13 wt %) behaves also in a similar way (Figure 9, e vs b).

As discussed above, the DMA/DSC experiments have shown that number of interesting processes including chemical cross-linking may take place in the PBA−PAN star copolymers at high temperatures. In order to study the effect of thermal treatment on the tensile properties of these materials, we have performed a number of quasi-static stress–strain experiments with the copolymer T-PBA388-PAN115. The results of these studies are shown in Figure 10. As can be seen, annealing at temperature of 200 °C for 30 min does not significantly change the tensile properties of the sample. However, annealing for only 10 min at temperature of 320 °C leads to a hardening and significant decrease in the ultimate tensile strength of the material. This effect can be related to the appearance of chemical cross-links that prevent stress distribution within the entangled chain network.[2] Similar behavior was observed by Tong and Jerome upon chemically cross-linking of the central block in PMMA−PBA−PMMA thermoplastic elastomers.[78] A further consequence of the high-temperature cross-linking is the fact that the T-PBA388-PAN115 sample annealed at 320 °C remains elastic until $\lambda = 2$ even at temperatures well above the softening point of PAN, as illustrated in Figure 8.

Conclusions

In summary, 3-arm star PBA−PAN block copolymers with low polydispersities were synthesized by ATRP with the aid of halogen exchange. A series of samples with different molecular weights and compositions were prepared. The morphology of solution-cast films of the 3-arm star PBA−PAN block copolymers was studied by tapping mode AFM and SAXS. Both techniques revealed a phase-separated morphology of cylindrical PAN domains hexagonally arranged in the pBA matrix. The mechanical and thermal properties of the star blocks have been thoroughly characterized by variety of techniques. We found that these materials possess typical elastomeric behavior in a broad range of service temperatures. Furthermore, their elastic moduli can be easily tuned to the values required for specific applications simply by adjusting the copolymer composition. The ultimate tensile strength was also found to strongly depend on the composition, i.e., to increase with the PAN content, however, remaining lower than those of the traditional SIPS thermoplastic elastomers. The 3-arm star PBA−PAN block copolymers retain their phase-separated morphology until temperatures of at least 250 °C. Because of chemical cross-linking of the PAN segments that takes places at higher temperatures, these materials preserve their elastomeric properties until temperatures of more than 300 °C. In this respect the 3-arm star PBA−PAN block copolymers have a much better thermal stability than the PMMA-based materials, in which the PMMA block depolymerizes at above 250 °C.

Acknowledgment. Support from the National Science Foundation (DMR 05-49353) is gratefully acknowledged. Many helpful discussions with Dr. J. Spanswick are acknowledged.

References and Notes

(1) Holden, G.; Bishop, E. T.; Legge, N. R. *J. Polym. Sci., Polym. Symp.* **1969**, *26*, 37–57.
(2) Holden, G.; Legge, N. R. In *Thermoplastic Elastomers*, 2nd ed.; Holden, G., Legge, N. R., Quirk, R. P., Schroeder, H. E., Eds.; Hanser: Munich, Germany, 1996; p 71.
(3) Fetters, L. J.; Morton, M. *Macromolecules* **1969**, *2*, 453–458.
(4) Morton, M. In *Thermoplastic Elastomers*; Holden, G., Schroeder, H. E., Eds.; Hanser: Munich, Germany, 1987; p 67.
(5) Jerome, R.; Fayt, R.; Teyssie, P. In *Thermoplastic Elastomers*; Legge, N. R., Holden, G., Schroeder, H. E., Eds.; Hanser: Munich, Germany, 1987; p 451.
(6) Yu, J. M.; Teyssie, P.; Jerome, R. *Macromolecules* **1996**, *29*, 8362–8370.
(7) Yu, Y. S.; Dubois, P.; Jerome, R.; Teyssie, P. *J. Polym. Sci., Part A: Polym. Chem.* **1996**, *34*, 2221–2228.
(8) Yu, J. M.; Dubois, P.; Jerome, R. *Macromolecules* **1996**, *29*, 7316–7322.
(9) Shim, J. S.; Asthana, S.; Omura, N.; Kennedy, J. P. *J. Polym. Sci., Part A: Polym. Chem.* **1998**, *36*, 2997–3012.
(10) Dair, B. J.; Honeker, C. C.; Alward, D. B.; Avgeropoulos, A.; Hadjichristidis, N.; Fetters, L. J.; Capel, M.; Thomas, E. L. *Macromolecules* **1999**, *32*, 8145–8152.
(11) Tsunogae, Y.; Kennedy, J. P. *J. Polym. Sci., Part A: Polym. Chem.* **1994**, *32*, 403–12.
(12) Kaszas, G.; Puskas, J. E.; Kennedy, J. P.; Hager, W. G. *J. Polym. Sci., Part A: Polym. Chem.* **1991**, *29*, 427–35.
(13) Duchacek, V. *J. Macromolecul. Sci., Phys.* **1998**, *B37*, 275–282.
(14) Feldthusen, J.; Ivan, B.; Mueller, A. H. E. *Macromolecules* **1998**, *31*, 578–585.
(15) Cao, X.; Faust, R. *Macromolecules* **1999**, *32*, 5487–5494.
(16) Tong, J. D.; Jerome, R. *Macromolecules* **2000**, *33*, 1479–1481.
(17) Tong, J. D.; Jerome, R. *Polymer* **1999**, *41*, 2499–2510.
(18) Tong, J. D.; Leclere, P.; Doneux, C.; Bredas, J. L.; Lazzaroni, R.; Jerome, R. *Polymer* **2000**, *41*, 4617–4624.
(19) Schmalz, H.; Abetz, V.; Lange, R.; Soliman, M. *Macromolecules* **2001**, *34*, 795–800.
(20) Ban, H. T.; Kase, T.; Kawabe, M.; Miyazawa, A.; Ishihara, T.; Hagihara, H.; Tsunogae, Y.; Murata, M.; Shiono, T. *Macromolecules* **2006**, *39*, 171–176.
(21) Braunecker, W. A.; Matyjaszewski, K. *Prog. Polym. Sci.* **2007**, *32*, 93–146.
(22) Tang, C. B.; Tracz, A.; Kruk, M.; Zhang, R.; Smilgies, D. M.; Matyjaszewski, K.; Kowalewski, T. *J. Am. Chem. Soc.* **2005**, *127*, 6918–6919.
(23) Tsarevsky, N. V.; Matyjaszewski, K. *Chem. Rev.* **2007**, *107*, 2270–2299.
(24) Matyjaszewski, K.; Xia, J. *Chem. Rev.* **2001**, *101*, 2921–2990.
(25) Matyjaszewski, K.; Davis, T. P. *Handbook of Radical Polymerization*; John Wiley & Sons: Hoboken, 2002.
(26) Hawker, C. J.; Bosman, A. W.; Harth, E. *Chem. Rev.* **2001**, *101*, 3661–3688.
(27) Chiefari, J.; Chong, Y. K.; Ercole, F.; Krstina, J.; Jeffery, J.; Le, T. P.; Mayadunne, R. T. A.; Meijs, G. F.; Moad, C. L.; Moad, G.; Rizzardo, E.; Thang, S. H. *Macromolecules* **1998**, *31*, 5559–5562.
(28) Kamigaito, M.; Ando, T.; Sawamoto, M. *Chem. Rev.* **2001**, *101*, 3689–3745.
(29) Davis, K. A.; Matyjaszewski, K. *Adv. Polym. Sci.* **2002**, *159*, 2–166.
(30) Patten, T. E.; Matyjaszewski, K. *Adv. Mater.* **1998**, *10*, 901–915.
(31) Wang, J.-S.; Matyjaszewski, K. *J. Am. Chem. Soc.* **1995**, *117*, 5614–15.
(32) Davis, K. A.; Matyjaszewski, K. *Macromolecules* **2001**, *34*, 2101–2107.
(33) Davis, K. A.; Paik, H.-j.; Matyjaszewski, K. *Macromolecules* **1999**, *32*, 1767–1776.
(34) Matyjaszewski, K.; Jo, S. M.; Paik, H.-j.; Shipp, D. A. *Macromolecules* **1999**, *32*, 6431–6438.
(35) Qiu, J.; Matyjaszewski, K. *Macromolecules* **1997**, *30*, 5643–5648.
(36) Teodorescu, M.; Matyjaszewski, K. *Macromol. Rapid Commun.* **2000**, *21*, 190–194.
(37) Tang, C.; Qi, K.; Wooley, K.; Matyjaszewski, K.; Kowalewski, T. *Angew. Chem., Int. Ed.* **2004**, *43*, 2783–2787.
(38) Moineau, C.; Minet, M.; Teyssie, P.; Jerome, R. *Macromolecules* **1999**, *32*, 8277–8282.
(39) Matyjaszewski, K.; Shipp, D. A.; McMurtry, G. P.; Gaynor, S. G.; Pakula, T. *J. Polym. Sci., Part A: Polym. Chem.* **2000**, *38*, 2023–2031.
(40) Robin, S.; Guerret, O.; Couturier, J.-L.; Pirri, R.; Gnanou, Y. *Macromolecules* **2002**, *35*, 3844–3848.

(41) Tsarevsky, N. V.; Sarbu, T.; Goebelt, B.; Matyjaszewski, K. *Macromolecules* **2002**, *35*, 6142–6148.
(42) Chatterjee, D. P.; Mandal, B. M. *Macromolecules* **2006**, *39*, 9192–9200.
(43) Rizzardo, E.; Chiefari, J.; Mayadunne, R. T. A.; Moad, G.; Thang, S. H. *ACS Symp. Ser.* **2000**, *768* (Controlled/Living Radical Polymerization), 278–296.
(44) Baumert, M.; Heinemann, J.; Thomann, R.; Mulhaupt, R. *Macromol. Rapid Commun.* **2000**, *21*, 271–276.
(45) Bielawski, C. W.; Morita, T.; Grubbs, R. H. *Macromolecules* **2000**, *33*, 678–680.
(46) Coelho, J. F. J.; Silva, A. M. F. P.; Popov, A. V.; Percec, V.; Abreu, M. V.; Goncalves, P. M. O. F.; Gil, M. H. *J. Polym. Sci., Part A: Polym. Chem.* **2006**, *44*, 3001–3008.
(47) Fonagy, T.; Ivan, B.; Szesztay, M. *Macromol. Rapid Commun.* **1998**, *19*, 479–483.
(48) Jankova, K.; Kops, J.; Chen, X.; Batsberg, W. *Macromol. Rapid Commun.* **1999**, *20*, 219–223.
(49) Mather, B. D.; Baker, M. B.; Beyer, F. L.; Berg, M. A. G.; Green, M. D.; Long, T. E. *Macromolecules* **2007**, *40*, 6834–6845.
(50) Miura, Y.; Kaneko, T.; Satoh, K.; Kamigaito, M.; Jinnai, H.; Okamoto, Y. *Chem.—Asian J.* **2007**, *2*, 662–672.
(51) Tong, J. D.; Leclere, P.; Doneux, C.; Bredas, J. L.; Lazzaroni, R.; Jerome, R. *Polymer* **2001**, *42*, 3503–3514.
(52) Yi, Y.; Fan, X.; Wan, X.; Li, L.; Zhao, N.; Chen, X.; Xu, J.; Zhou, Q.-F. *Macromolecules* **2004**, *37*, 7610–7618.
(53) Leclere, P.; Moineau, G.; Minet, M.; Dubois, P.; Jerome, R.; Bredas, J. L.; Lazzaroni, R. *Langmuir* **1999**, *15*, 3915–3919.
(54) Moineau, G.; Minet, M.; Teyssie, P.; Jerome, R. *Macromol. Chem. Phys.* **2000**, *201*, 1108–1114.
(55) Tong, J. D.; Moineau, G.; Leclere, P.; Bredas, J. L.; Lazzaroni, R.; Jerome, R. *Macromolecules* **2000**, *33*, 470–479.
(56) Storey, R. F.; Chrisholm, B. J.; Choate, K. R. *J. Polym. Sci., Part A: Polym. Chem.* **1994**, *34*, 2003–2017.
(57) Storey, R. F.; Shoemake, K. A. *J. Polym. Sci., Part A: Polym. Chem.* **1998**, *36*, 471–483.
(58) Shim, J. S.; Kennedy, J. P. *J. Polym. Sci., Part A: Polym. Chem.* **1999**, *37*, 815–824.
(59) Shim, J. S.; Kennedy, J. P. *J. Polym. Sci., Part A: Polym. Chem.* **2000**, *38*, 279–290.
(60) Davis, K. A.; Matyjaszewski, K. *Chin. J. Polym. Sci.* **2004**, *22*, 195–204.
(61) Matyjaszewski, K.; Shipp, D. A.; Wang, J.-L.; Grimaud, T.; Patten, T. E. *Macromolecules* **1998**, *31*, 6836–6840.
(62) Kowalewski, T.; McCullough, R. D.; Matyjaszewski, K. *Eur. Phys. J. E* **2003**, *10*, 5–16.
(63) Kowalewski, T.; Tsarevsky, N. V.; Matyjaszewski, K. *J. Am. Chem. Soc.* **2002**, *124*, 10632–10633.
(64) Tang, C.; Dufour, B.; Kowalewski, T.; Matyjaszewski, K. *Macromolecules* **2007**, *40*, 6199–6205.
(65) Chen, J.-T.; Shin, K.; Leiston-Belanger, J. M.; Zhang, M.; Russell, T. P. *Adv. Funct. Mater.* **2006**, *16*, 1476–1480.
(66) Keller, R. N.; Wycoff, H. D. *Inorg. Synth.* **1946**, *2*, 1–4.
(67) Matyjaszewski, K.; Patten, T. E.; Xia, J. *J. Am. Chem. Soc.* **1997**, *119*, 674–680.
(68) Huang, J.; Jia, S.; Siegwart, D. J.; Kowalewski, T.; Matyjaszewski, K. *Macromol. Chem. Phys.* **2006**, *207*, 801–811.
(69) Matyjaszewski, K. *Polym. Int.* **2003**, *52*, 1559–1565.
(70) Tang, C.; Kowalewski, T.; Matyjaszewski, K. *Macromolecules* **2003**, *36*, 1465–1473.
(71) Cleveland, J. P.; Anczykowski, B.; Schmid, A. E.; Elings, V. B. *Appl. Phys. Lett.* **1998**, *72*, 2613–2615.
(72) Wu, W.; Matyjaszewski, K.; Kowalewski, T. *Langmuir* **2005**, *21*, 1143–1148.
(73) Helfand, E.; Wasserman, Z. R. *Macromolecules* **1976**, *9*, 879–888.
(74) Leibler, L. *Macromolecules* **1980**, *13*, 1602–1617.
(75) Floudas, G.; Pakula, T.; Fischer, E. W.; Hadjichristidis, N.; Pispas, S. *Acta Polym.* **1994**, *45*, 176–181.
(76) Floudas, G.; Pakula, T.; Velis, G.; Sioula, S.; Hadjichristidis, N. *J. Chem. Phys.* **1998**, *108*, 6498–6501.
(77) Floudas, G.; Vlassopoulos, D.; Pitsikalis, M.; Hadjichristidis, N.; Stamm, M. *J. Chem. Phys.* **1996**, *104*, 2083–2088.
(78) Tong, J. D.; Jerome, R. *Polymer* **2000**, *41*, 2499–2510.
(79) Tong, J. D.; Leclere, P.; Rasmont, A.; Bredas, J. L.; Lazzaroni, R.; Jerome, R. *Macromol. Chem. Phys.* **2000**, *201*, 1250–1258.
(80) Matsen, M. W. *Phys. Rev. Lett.* **1998**, *80*, 4470–4473.
(81) Floudas, G.; Ulrich, R.; Wiesner, U. *J. Chem. Phys.* **1999**, *110*, 652–663.
(82) Floudas, G.; Ulrich, R.; Wiesner, U.; Chu, B. *Europhys. Lett.* **2000**, *50*, 182–188.

MA702561B